

CERN-TH/97-206

SWAT 97/159

hep-ph/9709213

TESTING TARGET INDEPENDENCE OF THE ‘PROTON SPIN’ EFFECT
IN SEMI-INCLUSIVE DEEP INELASTIC SCATTERING

G.M. Shore* and G. Veneziano†

* *Department of Physics
University of Wales Swansea
Singleton Park
Swansea, SA2 8PP, U.K.*

† *Theory Division
CERN
CH 1211 Geneva 23, Switzerland*

Abstract

A natural consequence of the composite operator propagator-vertex description of deep inelastic scattering developed by the authors is that the anomalous suppression observed in the flavour singlet contribution to the first moment of the polarised proton structure function g_1^p (the ‘proton spin’ problem) is not a special property of the proton structure but is a target independent effect which can be related to an anomalous suppression in the QCD topological susceptibility. In this paper, it is shown how this target independent mechanism can be tested in semi-inclusive deep inelastic scattering in which a pion or D meson carrying a large target energy fraction z is detected in the target fragmentation region.

CERN-TH/97-206

SWAT 97/159

August 1997

1. Introduction

The anomalous suppression of the first moment, Γ_1^p , of the polarised proton structure function g_1^p has been the focus of intense theoretical and experimental activity for nearly a decade. While it is now generally accepted that the key to understanding this effect is the existence of the chiral $U(1)$ anomaly in the flavour singlet pseudovector channel, there are several detailed explanations reflecting different theoretical approaches to the description of deep inelastic scattering (DIS) and proton structure. In this paper, we review one of these – the composite operator propagator-vertex (CPV) description of deep inelastic scattering developed by us in a series of papers[1-4] – and show how one of its key predictions, the target independence of the suppression mechanism, can be tested in future semi-inclusive DIS experiments.

The essence of our approach is the decomposition of structure function moments into the product of perturbative Wilson coefficients, non-perturbative but target-independent composite operator propagators, and vertex functions describing the coupling of these operators to the target nucleon.

The vertices, which are defined to be ‘1PI’ with respect to a chosen set of operators, encode all the information on the structure and properties of the target. They are non-perturbative and not directly calculable, and play the same role in our formalism as the parton densities in the conventional QCD parton model description of DIS. However, just as the parton densities have a universal character, being equally applicable to DIS or hadron-hadron scattering, these 1PI vertices also have a more universal role, being related in favourable cases to low energy nucleon couplings such as $g_{\pi NN}$ etc. They provide an alternative, complementary, description of the nucleon state.

However, the most important feature of the CPV formalism as far as the ‘proton spin’ problem is concerned is the separation of the composite operator propagator from the target-dependent vertex. This allows us to distinguish between generic non-perturbative properties of QCD and effects which are characteristic of the particular target. Our proposal is that the anomalous suppression in the flavour singlet contribution to the first moment of g_1^p is of the first kind, viz. a generic, *target-independent* feature of QCD, related to the chiral $U(1)$ anomaly but not special to any particular hadron. In fact[1-3], we are able to relate the relevant propagator to a fundamental correlation function in QCD, viz. the topological susceptibility $\chi(0)$, and show that the suppression in Γ_1^p is due to an anomalously small value of its first moment $\chi'(0)$. To confirm this interpretation, we have evaluated $\chi'(0)$ using QCD spectral sum rules[4], and have found a suppression in good quantitative agreement with the current data[5,6] on g_1^p .

The natural next step is to see whether this target-independent suppression mechanism can be tested directly, by studying the structure functions of other targets besides the proton and neutron. (Unfortunately, for these two targets, isospin invariance already implies target independence.) The obvious choice for an alternative target is the photon, whose structure function g_1^γ may be measured in two-photon processes at a sufficiently high-luminosity e^+e^- collider. However, this turns out to be an exceptional case, since there is a direct axial current – two photon coupling via the electromagnetic chiral $U(1)$ anomaly. The first moment sum rule for $g_1^\gamma(k^2)$, as a function of the target photon virtuality k^2 ,

has been presented in refs.[7,8], together with estimates of the relevant cross-section asymmetries in polarised colliders. The dependence of $g_1^\gamma(k^2)$ on the virtuality displays many interesting features: $g_1^\gamma(0)$ is zero by electromagnetic current conservation[9]; its asymptotic value for k^2 greater than the hadronic scale is essentially given by the electromagnetic anomaly coefficient, with logarithmic corrections governed by the gluonic anomaly; and its detailed dependence on k^2 as the various quark thresholds are crossed depends critically on the realisation of chiral symmetry in QCD.

Direct DIS experiments on other hadronic targets are of course not feasible. We can nevertheless test our ideas in *semi-inclusive* DIS in an appropriate kinematic region where the reaction is well described in terms of deep inelastic photon scattering off a Reggeon (or more complicated exchanged object) with well-defined hadronic characteristics. In particular, using the target-independent suppression hypothesis, we are able to formulate predictions for ratios of cross section moments (related to moments of the Reggeon structure functions) which are significantly and characteristically different from expectations based, like the Ellis-Jaffe sum rule for g_1^p , on the simple valence quark model or OZI rule. In particular, our target-independent mechanism should be clearly testable by comparing the ratios of cross section moments for the semi-inclusive reactions $ep \rightarrow e\pi^-(D^-)X$ and $en \rightarrow e\pi^+(D^0)X$, in which a pion or D meson carrying a large target energy fraction z is detected in the target fragmentation region.

The paper is organised as follows. In section 2, we review the most important features of the CPV method and its application to the polarised proton structure function, explain why it leads to a target-independent suppression, and compare our prediction for the first moment with the most recent SMC data. Then, in section 3, we show how by assuming target-independence and exploiting flavour $SU(3)$ symmetry we can derive predictions for ratios of structure function moments for a variety of hadrons, including some which differ dramatically from results using the OZI rule.

Semi-inclusive DIS is introduced in section 4, where we use a combination of symmetry and dynamical arguments to show that our predictions for ratios of structure function moments can be realised as ratios of cross section moments in a certain kinematical region. In this region, the cross sections may be written in terms of Reggeon structure functions, where the exchanged Regge trajectory has the required $SU(3)$ properties. We then compare these results with the more precise description of semi-inclusive DIS in terms of fracture functions[10], and relate the Reggeon structure function to the recently introduced extended fracture functions[11]. We conclude with a summary of our predictions for the most interesting ratios of semi-inclusive cross sections.

2. Target Independence and Composite Operator Propagator-Vertex Method

The starting point is the sum rule for the first moment of the polarised structure function g_1^p , viz.

$$\begin{aligned}\Gamma_1^p(Q^2) &\equiv \int_0^1 dx g_1^p(x; Q^2) \\ &= \frac{1}{12} C_1^{\text{NS}}(\alpha_s(Q^2)) \left(a^3 + \frac{1}{3} a^8 \right) + \frac{1}{9} C_1^{\text{S}}(\alpha_s(Q^2)) a^0(Q^2)\end{aligned}\quad (2.1)$$

Here, a^3 , a^8 and $a^0(Q^2)$ are the form factors in the forward proton matrix elements of the renormalised axial current, i.e.

$$\langle p, s | A_\mu^3 | p, s \rangle = s_\mu \frac{1}{2} a^3 \quad \langle p, s | A_\mu^8 | p, s \rangle = s_\mu \frac{1}{2\sqrt{3}} a^8 \quad \langle p, s | A_\mu^0 | p, s \rangle = s_\mu a^0(Q^2)\quad (2.2)$$

where p_μ and s_μ are the momentum and polarisation vector of the proton. The Q^2 dependence of the singlet form factor follows from the renormalisation of the singlet current described below. The perturbative series $C_1^{\text{NS}}(\alpha_s(Q^2))$ and $C_1^{\text{S}}(\alpha_s(Q^2))$ are OPE coefficients and are now both known to $O(\alpha_s^3)$ [12-14].

Because of the chiral $U(1)$ anomaly, the singlet current A_μ^0 is renormalised and mixes with the topological density. Defining the bare operators $A_{\mu B}^0 = \sum \bar{q} \gamma_\mu \gamma_5 q$ and $Q_B = \frac{\alpha_s}{8\pi} \epsilon^{\mu\nu\rho\sigma} \text{tr} G_{\mu\nu} G_{\rho\sigma}$, we have (for n_f flavours)

$$\begin{aligned}A_\mu^0 &= Z A_{\mu B}^0 \\ Q &= Q_B - \frac{1}{2n_f} (1 - Z) \partial^\mu A_{\mu B}^0\end{aligned}\quad (2.3)$$

where Z is a divergent renormalisation constant. The associated anomalous dimension γ was first calculated in ref.[15] and is now known to 3 loops[16]. Matrix elements of A_μ^0 therefore have a non-trivial scale dependence governed by γ . In particular,

$$\frac{d}{dt} a^0 = \gamma a^0\quad (2.4)$$

where $t = \ln \frac{Q^2}{\Lambda^2}$.

The anomalous Ward identities for composite operator propagators are

$$\partial^\mu \langle 0 | T A_\mu^0 \mathcal{O} | 0 \rangle - 2n_f \langle 0 | T Q \mathcal{O} | 0 \rangle = \langle \delta_A \mathcal{O} \rangle\quad (2.5)$$

where \mathcal{O} denotes an arbitrary composite operator and $\delta_A \mathcal{O}$ is its chiral variation. Notice that with these definitions of the renormalised composites, the combination $(\partial^\mu A_\mu^0 - 2n_f Q)$ appearing in the anomalous Ward identities is the same for the bare or renormalised

operators[17]. The possibility of making such a definition is a consequence of the Adler-Bardeen theorem.

The sum rule (2.1) is derived using the OPE for two electromagnetic currents. The dominant contributions arise from the operators of lowest twist and, within this set, those of spin n contribute to the n th moment of the relevant structure function. Eq.(2.1) is the special case for odd parity operators of twist 2 and spin 1, viz.

$$J^\rho(q)J^\sigma(-q) \underset{Q^2 \rightarrow \infty}{\sim} 2\epsilon^{\rho\sigma\nu\mu} \frac{q_\nu}{Q^2} \left[C_1^{\text{NS}}(\alpha_s(Q^2)) \left(A_\mu^3 + \frac{1}{\sqrt{3}} A_\mu^8 \right) + \frac{2}{3} C_1^{\text{S}}(\alpha_s(Q^2)) A_\mu^0 \right] \quad (2.6)$$

It is at this point that our CPV method and the conventional parton model analysis of DIS diverge. In the parton model, the form factors are related to quark and gluon densities as follows[18]:

$$\begin{aligned} a^3 &= \Delta u - \Delta d \\ a^8 &= \Delta u + \Delta d - 2\Delta s \\ a^0(Q^2) &= \Delta\Sigma - n_f \frac{\alpha_s(Q^2)}{2\pi} \Delta g(Q^2) \end{aligned} \quad (2.7)$$

where $\Delta\Sigma = \Delta u + \Delta d + \Delta s$ and $\Delta q = \int_0^1 dx (\Delta q(x) + \Delta \bar{q}(x))$. There is a scheme ambiguity in these identifications, which relate four parton densities to just three measured quantities. The above definitions, in which $\Delta\Sigma$ is chosen to be scale invariant to all orders (this is possible because of the Adler-Bardeen theorem), are made in the AB factorisation scheme[18-20].

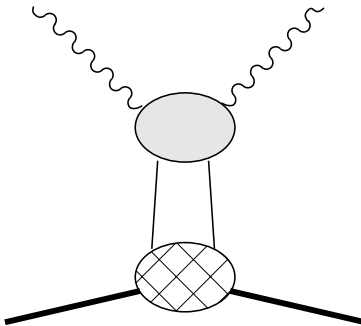


Fig. 1: The description of DIS in the parton model. The upper hatched blob denotes the perturbative QCD corrections related to the Wilson coefficients in the OPE.

This standard approach is illustrated in Fig. 1. The upper hatched blob represents the perturbative QCD corrections contributing to the coefficient functions $C_1^{\text{NS}}, C_1^{\text{S}}$ in the OPE. The factorisation theorems show that these diagrams, with two quark (gluon) propagators, give the leading contribution to the amplitude for large Q^2 , thus allowing the simple parton interpretation of $q(x)$ and $g(x, t)$ as the probability distributions for finding a quark or gluon with momentum fraction x in the target proton.

The Ellis-Jaffe sum rule makes the assumption that Δs and Δg are zero in the proton. This is equivalent to the OZI (Zweig) rule prediction $a^0 = a^8$. The crux of the ‘proton

spin' problem is to understand the origin of the OZI breaking revealed by the measurement of Γ_1^p , which shows that a^0 is strongly suppressed relative to its OZI value. Our favoured explanation in the context of the parton model is that the OZI breaking is due overwhelmingly to the gluon density Δg in eq.(2.7). We expect the OZI rule to apply to the scale invariant quark densities, so that (in the AB scheme) $\Delta\Sigma = a^8$, while the scale dependent $\Delta g(Q^2)$ compensates to produce an anomalously suppressed $a^0(Q^2)$. This would accord with the central conjecture of our rather different approach, described below, and has the virtue of providing a scale invariant meaning to the OZI rule in the presence of the chiral $U(1)$ anomaly.

In our approach, we again start from the OPE but instead factorise the resulting matrix elements into the product of composite operator propagators and vertex functions.⁽¹⁾

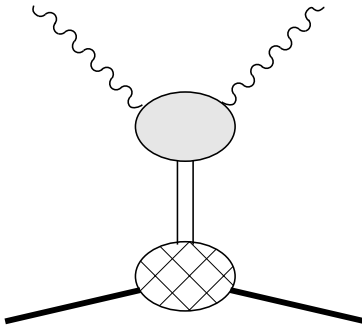


Fig. 2: The description of DIS in the composite operator propagator-vertex method. The double line denotes the composite operator propagator and the lower cross-hatched blob the ‘1PI’ vertex function.

This is illustrated in Fig. 2. To do this, we first select a set of composite operators $\tilde{\mathcal{O}}_i$ appropriate (see below) to the physical situation and define vertices $\Gamma_{\tilde{\mathcal{O}}_i pp}$ as ‘1PI’ with respect to this set. Technically, this is achieved by introducing sources for these operators in the QCD generating functional, then performing a Legendre transform to obtain an effective action $\Gamma[\tilde{\mathcal{O}}_i]$. The 1PI vertices are the functional derivatives of $\Gamma[\tilde{\mathcal{O}}_i]$. A generic structure function sum rule then takes the form

$$\int_0^1 dx x^{n-1} F(x, Q^2) = \sum_i \sum_j C_j^{(n)}(Q^2) \langle 0|T \mathcal{O}_j^{(n)} \tilde{\mathcal{O}}_i|0\rangle \Gamma_{\tilde{\mathcal{O}}_i pp} \quad (2.8)$$

where $\mathcal{O}_j^{(n)}$ are the lowest twist, spin n , operators in the appropriate OPE with $C_j^{(n)}$ the corresponding Wilson coefficients.

This decomposition splits the structure function into three pieces – first, the Wilson coefficients $C_j^{(n)}(Q^2)$ which control the Q^2 dependence and can be calculated in perturbative QCD; second, non-perturbative but *target-independent* QCD correlation functions (composite operator propagators) $\langle 0|T \mathcal{O}_j^{(n)} \tilde{\mathcal{O}}_i|0\rangle$; and third, a non-perturbative, target-dependent vertex functions $\Gamma_{\tilde{\mathcal{O}}_i pp}$ describing the coupling of the target proton to the composite operators of interest. The vertex functions cannot be calculated directly from first

⁽¹⁾ The presentation here is a slight over-simplification. In general, there is a distinction between the cases where the OPE operators \mathcal{O}_j are included in the set $\tilde{\mathcal{O}}_i$ and where they are not. See refs.[2,3] for a complete account of the Zumino (partial Legendre) transform formalism and its application to the ‘proton spin’ problem.

principles. They encode the information on the nature of the proton state and play an analogous role to the parton distributions in the more conventional parton picture.

One of the main advantages of our method is that some non-perturbative information which is generic to QCD, i.e. independent of the target, is factored off into the composite operator propagator. This allows us to distinguish between non-perturbative mechanisms which are generic to all QCD processes and those which are specific to a particular target. Our contention is that the anomalous suppression in the first moment of g_1^p is of the first, target-independent, type.

As emphasised in refs.[3,4,21,22], it is important to recognise that this decomposition of the matrix elements into products of propagators and proper vertices is *exact*, independent of the choice of the set of operators $\tilde{\mathcal{O}}_i$. In particular, it is not necessary for $\tilde{\mathcal{O}}_i$ to be in any sense a complete set. All that happens if a different choice is made is that the vertices $\Gamma_{\tilde{\mathcal{O}}_i pp}$ themselves change, becoming ‘1PI’ with respect to a different set of composite fields. Of course, while any set of $\tilde{\mathcal{O}}_i$ may be chosen, some will be more convenient than others. Clearly, the set of operators should be as small as possible while still capturing the essential physics (i.e. they should encompass the relevant degrees of freedom) and indeed a good choice can result in vertices $\Gamma_{\tilde{\mathcal{O}}_i pp}$ which are both RG invariant and closely related to low energy physical couplings, such as $g_{\pi NN}$ or $g_{\pi\gamma\gamma}$ [3,23]. In this case, eq.(2.8) provides a rigorous relation between high Q^2 DIS and low-energy meson-nucleon scattering.

For the first moment sum rule for g_1^p , it is most convenient to use the chiral anomaly immediately to re-express $a^0(Q^2)$ in terms of the forward matrix element of the topological density Q , i.e.

$$a^0(Q^2) = \frac{1}{2M} 2n_f \langle p|Q|p\rangle \quad (2.9)$$

where the matrix element, which scales with the anomalous dimension γ , is evaluated at the scale Q^2 .⁽²⁾

Our set of operators $\tilde{\mathcal{O}}_i$ is then chosen to be the renormalised flavour singlet pseudoscalars Q and Φ_5 where, up to a vital normalisation factor, the corresponding bare operator is $\Phi_{5B} = \sum \bar{q}\gamma_5 q$. The normalisation factor[3,4] is chosen such that in the absence of the anomaly⁽³⁾, Φ_5 would have the correct normalisation to couple with unit decay constant to the $U(1)$ Goldstone boson which would exist in this limit. This is important

⁽²⁾ This quantity may be evaluated directly in lattice QCD. See ref.[24] for a brief review of the current status of lattice evaluations. Note that in order to incorporate fully the effects of the anomaly, it is necessary[25] to use dynamical fermions.

⁽³⁾ To be precise, what is referred to here is the ‘OZI limit’ of QCD, defined in ref.[25] as the truncation of full QCD in which non-planar and quark-loop diagrams are retained, but diagrams in which the external currents are attached to distinct quark loops (so that there are purely gluonic intermediate states) are omitted. This is a more accurate approximation to full QCD than either the leading large $1/N_c$ limit, the quenched approximation (small n_f at fixed N_c) or the leading topological expansion ($N_c \rightarrow \infty$ at fixed n_f/N_c). In the OZI limit, the $U(1)$ anomaly is absent, as is meson-gluon mixing[26], and there is an extra $U(1)$ Goldstone boson. Notice, however, that no approximation is used in deriving eq.(2.10). The OZI limit is used here purely as the motivation for choosing a particularly convenient normalisation for Φ_5 .

later in justifying the use of the OZI approximation for the vertex, which is then RG invariant.

We then have

$$\Gamma_{1 \text{ singlet}}^p = \frac{1}{9} \frac{1}{2M} 2n_f C_1^S(\alpha_s(Q^2)) \left[\langle 0|T Q Q|0\rangle \Gamma_{Qpp} + \langle 0|T Q \Phi_5|0\rangle \Gamma_{\Phi_5pp} \right] \quad (2.10)$$

where the propagators are at zero momentum and the vertices (which in this equation have the external proton wave functions amputated) are 1PI wrt Q and Φ_5 only.

The composite operator propagator in the first term is the zero-momentum limit of the QCD topological susceptibility $\chi(k^2)$, viz.

$$\chi(k^2) = \int dx e^{ik \cdot x} i \langle 0|T Q(x) Q(0)|0\rangle \quad (2.11)$$

The anomalous chiral Ward identities show that $\chi(0)$ vanishes for QCD with massless quarks, in contrast to pure Yang-Mills theory where $\chi(0)$ is non-zero. Furthermore, it can be shown[3,4] that the propagator $\langle 0|T Q \Phi_5|0\rangle$ at zero momentum is simply the square root of the first moment of the topological susceptibility. We therefore find:

$$\Gamma_{1 \text{ singlet}}^p = \frac{1}{9} \frac{1}{2M} 2n_f C_1^S(\alpha_s(Q^2)) \sqrt{\chi'(0)} \Gamma_{\Phi_5pp} \quad (2.12)$$

The quantity $\sqrt{\chi'(0)}$ is not RG invariant and scales with the anomalous dimension γ . On the other hand, the proper vertex has been chosen specifically so as to be RG invariant. The renormalisation group properties of this decomposition are crucial to our resolution of the ‘proton spin’ problem.

Our proposal (which is fully motivated in refs.[3,23] and supported by a range of low-energy phenomenology in the $U(1)$ channel, such as $\eta' \rightarrow \gamma\gamma$ decay) is that we should expect the source of OZI violations to lie in the RG non-invariant, and therefore anomaly-sensitive, terms, i.e. in $\chi'(0)$.⁽⁴⁾ Since the anomalous suppression in Γ_1^p is assigned to the composite operator propagator rather than the proper vertex, the suppression is a target independent property of QCD related to the chiral anomaly, not a special property of the proton structure. This immediately raises the question whether it is possible to test the mechanism by effectively performing DIS experiments on other hadronic targets.

Our quantitative prediction then follows by using the OZI approximation for the vertex Γ_{Φ_5pp} and a QCD spectral sum rule estimate of the first moment of the topological susceptibility.⁽⁵⁾ We find, for $n_f = 3$,

$$\sqrt{\chi'(0)} \Big|_{Q^2=10GeV^2} = 23.2 \pm 2.4 \text{ MeV} \quad (2.13)$$

⁽⁴⁾ Notice that we are using RG non-invariance, i.e. dependence on the anomalous dimension γ , merely as an indicator of which quantities are sensitive to the anomaly and therefore likely to show OZI violations. An alternative suggestion, in which the suppression in $a^0(Q^2)$ is due directly to non-perturbative effects in γ at low scales, was made in ref. [27]. This would also predict a target-independent suppression.

⁽⁵⁾ The validity of this calculation has been criticised by Ioffe[28,29] (see also ref.[30,31]), who asserts that the spectral sum rule technique cannot be applied to the $U(1)$ channel because of problems with the optimisation scale and dependence on the strange quark mass. In ref.[32], we extend our analysis to include light quark masses and explain in detail why these criticisms are not valid.

This is a suppression of approximately a factor 0.6 relative to the OZI value $f_\pi/\sqrt{6}$.

Our final result is then

$$a^0(Q^2 = 10\text{GeV}^2) = 0.35 \pm 0.05 \quad (2.14)$$

from which we deduce

$$\Gamma_1^p \Big|_{Q^2=10\text{GeV}^2} = 0.143 \pm 0.005 \quad (2.15)$$

This is to be compared with the Ellis-Jaffe (OZI) prediction of $a^0 = 0.58 \pm 0.02$ and the SMC experimental data[5]:

$$\Gamma_1^p \Big|_{Q^2=10\text{GeV}^2} = 0.136 \pm 0.013 \pm 0.009 \pm 0.005 \quad (2.16)$$

where the last error is theoretical, related to the Q^2 evolution. This gives

$$a^0(Q^2 = 10\text{GeV}^2) = 0.28 \pm 0.16 \quad (2.17)$$

There is, however, a remaining uncertainty over the data related to the small x region. The SMC experiment is limited to measuring the region $0.003 < x < 0.7$, and only a small estimated contribution of 0.0042 ± 0.0016 is included in eq.(2.16) for the contribution to Γ_1^p from the unmeasured range $0 < x < 0.003$. (The high x extrapolation is uncontroversial.) Recent fits[19,33] to the same data using a different extrapolation to the small x region, incorporating Q^2 evolution of the parton distributions, suggest a much smaller central value for a^0 with larger errors, viz. $a^0(Q^2 = 10\text{GeV}^2) = 0.10^{+0.17}_{-0.11}$. Interestingly, these fits also suggest that $\Delta\Sigma = 0.45 \pm 0.09$, not too far from the OZI value.

Very recently, new preliminary proton data has become available from SMC[6]. This gives

$$\int_{0.003}^1 dx g_1^p(x; Q^2 = 10\text{GeV}^2) = 0.146 \pm 0.006 \pm 0.009 \pm 0.005 \quad (2.18)$$

The result for the entire first moment depends on how the extrapolation to the unmeasured small x region is performed. Using a simple Regge fit, SMC find $\Gamma_1^p = 0.149 \pm 0.012$ from which $a^0 = 0.41 \pm 0.11$, while using a small x fit using perturbative QCD evolution of the parton distributions they find $\Gamma_1^p = 0.135 \pm 0.016$ which implies $a^0 = 0.27 \pm 0.15$ (all at $Q^2 = 10\text{GeV}^2$).

Clearly, much more analysis, both theoretical and experimental, of the small x behaviour of the polarised structure functions is required and studying this region will be an important goal of future polarised collider experiments at HERA. Nevertheless, the broad agreement with our prediction (2.14) is very encouraging and strongly suggests that our interpretation and explicit calculation of the topological susceptibility are correct.

3. The g_1 Sum Rule for Other Targets

In this section, we consider the implications of the target-independent suppression mechanism for the structure functions of other hadrons, leaving aside temporarily the question of how this may be realised experimentally.

Our basic prediction⁽⁶⁾ is that for any hadron, the singlet form factor in eq.(2.1) can be substituted by its OZI value multiplied by a universal (target-independent) suppression factor $s(Q^2)$ determined, up to radiative corrections, by the anomalous suppression of the first moment of the topological susceptibility $\sqrt{\chi'(0)}$. For example, for a hadron containing only u and d quarks, the OZI relation is simply $a^0 = a^8$, so we would predict:

$$\Gamma_1^p = \frac{1}{12} C_1^{\text{NS}}(\alpha_s(Q^2)) \left(a^3 + \frac{1}{3}(1 + 4s)a^8 \right) \quad (3.1)$$

where

$$s(Q^2) = \frac{C_1^{\text{S}}(\alpha_s(Q^2))}{C_1^{\text{NS}}(\alpha_s(Q^2))} \frac{a^0(Q^2)}{a^8} \quad (3.2)$$

Since s is target independent, we can use the value measured for the proton to deduce Γ_1 for any other hadron target simply from the flavour non-singlet form factors, which obey relations from flavour $SU(3)$ symmetry. From our spectral sum rule estimate of $\sqrt{\chi'(0)}$, we find $s \sim 0.66$ at $Q^2 = 10\text{GeV}^2$, while the central value of the SMC result (2.17) gives $s \sim 0.55$. (We use the experimental data taken directly from SMC, ref.[5] in this section.)

The form factors for a hadron \mathcal{B} are given by the matrix elements of the flavour octet axial currents. The $SU(3)$ properties are summarised by

$$\langle \mathcal{B} | A_{II_3 Y}^{(\rho)} | \mathcal{B} \rangle = \langle I^{\mathcal{B}} I_3^{\mathcal{B}}; I^{\bar{\mathcal{B}}} I_3^{\bar{\mathcal{B}}} | II_3 \rangle \left(\begin{array}{cc|cc} \rho^{\mathcal{B}} & \rho^{\bar{\mathcal{B}}} & & \\ I^{\mathcal{B}} & Y^{\mathcal{B}} & I^{\bar{\mathcal{B}}} & Y^{\bar{\mathcal{B}}} \end{array} \middle| \begin{array}{cc} \rho & \\ I & Y \end{array} \right) \langle \rho^{\mathcal{B}} | A^{(\rho)} | \rho^{\mathcal{B}} \rangle \quad (3.3)$$

Here, ρ indicates the $SU(3)$ representation while I, I_3 and Y are the isospin and hypercharge quantum numbers. The term $\langle \rho^{\mathcal{B}} | A^{(\rho)} | \rho^{\mathcal{B}} \rangle$ is a reduced matrix element, while the other factors are $SU(2)$ and $SU(3)$ Clebsch-Gordon coefficients[36].

If we now take the hadron \mathcal{B} to be in the $\mathbf{10}$ representation, then since

$$\mathbf{10} \times \bar{\mathbf{10}} = \mathbf{1} + \mathbf{8} + \mathbf{27} + \mathbf{64} \quad (3.4)$$

⁽⁶⁾ The analogous prediction in the parton model would be to assume that (in the AB scheme) the RG invariant $\Delta\Sigma$ would take its OZI value, ie. $\Delta\Sigma \simeq \Delta\Sigma_{val}$, where $\Delta\Sigma_{val}$ is the sum of the valence quark densities. These can be distinguished from the OZI-violating sea quark densities in semi-inclusive DIS in the current fragmentation region[34,35]. The gluon contribution $\Delta G \equiv n_f \frac{\alpha_s(Q^2)}{2\pi} \Delta g(Q^2)$ would then be given by

$$\Delta G = (1 - \tilde{s}(Q^2)) \Delta\Sigma_{val}$$

where $\tilde{s}(Q^2)$ is simply (3.2) with the Wilson coefficients omitted. This has the correct scaling property and ensures a target independent suppression in Γ_1 .

the matrix element of the (octet) currents contain just one reduced matrix element. This is in contrast to the case of \mathcal{B} in the octet representation, as for the proton or neutron, which would involve an F/D ratio arising from the two reduced matrix elements in the decomposition $\mathbf{8} \times \mathbf{8} = \mathbf{1} + \mathbf{8} + \mathbf{8} + \mathbf{10} + \overline{\mathbf{10}} + \mathbf{27}$. This is an important simplification, as it means that the ratio of Γ_1 for decuplet states can be predicted as a simple group-theoretic number, up to the dynamical suppression factor s .

For example, for the Δ^{++} , the matrix elements of the currents are

$$\langle \Delta^{++} | A_\mu^3 | \Delta^{++} \rangle = \sqrt{\frac{3}{10}} \langle \mathbf{10} | A^{(\mathbf{8})} | \mathbf{10} \rangle \quad \langle \Delta^{++} | A_\mu^8 | \Delta^{++} \rangle = \sqrt{\frac{1}{10}} \langle \mathbf{10} | A^{(\mathbf{8})} | \mathbf{10} \rangle \quad (3.5)$$

evaluating the relevant Clebsch-Gordon coefficients. Similar results hold for the Δ^- . Taking the ratio to eliminate the common reduced matrix element $\langle \mathbf{10} | A^{(\mathbf{8})} | \mathbf{10} \rangle$, we find the following result for the ratio of the first moment of the polarised structure functions g_1 for the Δ^{++} and Δ^- :

$$\frac{\Gamma_1^{\Delta^{++}}}{\Gamma_1^{\Delta^-}} = \frac{\sqrt{\frac{3}{10}} + \sqrt{\frac{1}{10}} \sqrt{\frac{1}{3}} (1 + 4s)}{-\sqrt{\frac{3}{10}} + \sqrt{\frac{1}{10}} \sqrt{\frac{1}{3}} (1 + 4s)} = \frac{2s + 2}{2s - 1} \quad (3.6)$$

The OZI (c.f. Ellis-Jaffe) prediction is given by setting $s = 1$, i.e. $\Gamma_1^{\Delta^{++}} / \Gamma_1^{\Delta^-} = 4$.⁽⁷⁾ However, substituting a suppression factor of $s \sim 0.66$ gives a much larger ratio $\Gamma_1^{\Delta^{++}} / \Gamma_1^{\Delta^-} \sim 10$, while the experimental factor $s \sim 0.55$ would give an even larger value, indicating a near complete suppression of $\Gamma_1^{\Delta^-}$.

We would therefore expect to find a quite spectacular deviation from the quark model expectation for this ratio of structure function moments. We can also show (footnote (7)) that the same result is obtained for the ratio $\Gamma_1^{\Sigma_c^{++}} / \Gamma_1^{\Sigma_c^0}$ for the charmed baryons $\Sigma_c^{++} = uuc$ and $\Sigma_c^0 = ddc$. Of course, these examples have been specially selected (because of the $2s - 1$ factor) to show a particularly striking difference from the simple valence quark model predictions. However, as we shall see in section 4, they are also the examples which can be dynamically isolated in semi-inclusive DIS.

Although these are the most interesting, other ratios of structure function moments can be easily calculated by the same method. The most obvious is the proton-neutron

⁽⁷⁾ Alternatively, this result can be simply obtained in the valence quark model as follows. Using the quark charges and neglecting radiative corrections, we have

$$\Gamma_1 = \frac{1}{18} (4\Delta u + \Delta d + \Delta s)$$

and so

$$\Gamma_1^{\Delta^{++}} = \frac{2}{3} \Delta u (\Delta^{++}) \quad \Gamma_1^{\Delta^-} = \frac{1}{6} \Delta d (\Delta^-)$$

With the (isospin) assumption $\Delta u (\Delta^{++}) = \Delta d (\Delta^-)$, we immediately find $\Gamma_1^{\Delta^{++}} / \Gamma_1^{\Delta^-} = 4$.

The corresponding result for the ratio $\Gamma_1^{\Sigma_c^{++}} / \Gamma_1^{\Sigma_c^0}$ follows from quark counting in the same way, assuming $\Delta u (\Sigma_c^{++}) = \Delta d (\Sigma_c^0)$ and treating the heavy c quark as a spectator.

ratio which, as noted above, does not simply give a group theoretic number but depends also on the F/D ratio. In this case, the OZI prediction is

$$\frac{\Gamma_1^p}{\Gamma_1^n} = \frac{1 - 9F/D}{4 - 6F/D} \quad (3.7)$$

while including the anomalous suppression factor, we find

$$\frac{\Gamma_1^p}{\Gamma_1^n} = \frac{2s - 1 - 3(2s + 1)F/D}{2s + 2 - 6sF/D} \quad (3.8)$$

This complements the Bjorken sum rule for the difference $\Gamma_1^p - \Gamma_1^n$, viz.

$$\Gamma_1^p - \Gamma_1^n = \frac{1}{6} C_1^{\text{NS}}(\alpha_s(Q^2)) g_A \quad (3.9)$$

where $g_A = a_p^3$. The neutron structure function is[5]

$$\Gamma_1^n \Big|_{Q^2=10\text{GeV}^2} = -0.046 \pm 0.021 \quad (3.10)$$

so that the experimental result for the ratio is

$$\frac{\Gamma_1^p}{\Gamma_1^n} \Big|_{Q^2=10\text{GeV}^2} = -2.96 \pm 1.39 \quad (3.11)$$

This is to be compared with the OZI result $\Gamma_1^p/\Gamma_1^n = -7.6 \pm 1.4$, where we have used $F/D = 0.575 \pm 0.016$ in eq.(3.7), and with the prediction from our modified formula (3.8) which gives central values $\Gamma_1^p/\Gamma_1^n = -3.5$ for $s \sim 0.66$ and $\Gamma_1^p/\Gamma_1^n = -2.9$ for $s \sim 0.55$. Of course, this only confirms that the suppression in the singlet form factor $a^0(Q^2)$ is the same for the proton and neutron, as expected by isospin symmetry and confirmed by the experimental validity of the Bjorken sum rule.

As a final example, we quote the corresponding results for hadrons containing the strange quark. For the octet Σ^+ and Σ^- , the OZI rule gives respectively $a^0 = \frac{1}{2}(3a^3 - a^8)$ and $a^0 = -\frac{1}{2}(3a^3 + a^8)$, so that our prediction is

$$\Gamma_1^{\Sigma^+} = \frac{1}{12} C_1^{\text{NS}}(\alpha_s(Q^2)) \left((1 + 2s)a^3 + \frac{1}{3}(1 - 2s)a^8 \right) \quad (3.12)$$

while

$$\Gamma_1^{\Sigma^-} = \frac{1}{12} C_1^{\text{NS}}(\alpha_s(Q^2)) \left((1 - 2s)a^3 + \frac{1}{3}(1 - 2s)a^8 \right) \quad (3.13)$$

A similar group theoretic calculation then gives

$$\frac{\Gamma_1^{\Sigma^+}}{\Gamma_1^{\Sigma^-}} = \frac{2s - 1 - 3(2s + 1)F/D}{2s - 1 - 3(2s - 1)F/D} \quad (3.14)$$

with the valence quark model prediction again being recovered by setting $s = 1$.

On the other hand, for the Σ^{*+} and Σ^{*-} in the decuplet, the F/D ratio is absent and instead we find the simple ratio

$$\frac{\Gamma_1^{\Sigma^{*+}}}{\Gamma_1^{\Sigma^{*-}}} = \frac{2s + 1}{2s - 1} \quad (3.15)$$

We shall see to what extent these predictions may be tested in the next section.

4. Semi-Inclusive Deep Inelastic Scattering

Of course, it is not possible to measure structure functions directly for baryonic targets such as the Δ or Σ_c . However, it is possible to test the ideas in the previous sections in semi-inclusive DIS reactions $eN \rightarrow ehX$, where h is a detected hadron in the target fragmentation region.

In our case, we are interested in reactions where N is a nucleon target and the detected hadron h is, for the interesting cases described above, a pion or D meson. The electron can of course represent any lepton. There are distinct contributions to this process from the current and target fragmentation regions, which we require to be clearly distinguished kinematically. A large rapidity gap is therefore required between h and the inclusive hadrons X , with h in the target fragmentation region. h is also required to carry a large target energy fraction z (defined below).

4.1 Single Reggeon Exchange Model

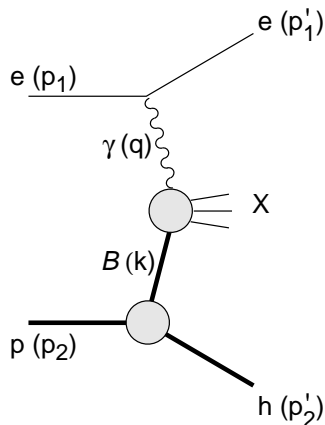


Fig.3 : The semi-inclusive DIS reaction $eN \rightarrow ehX$ in the target fragmentation region with $z \sim 1$ modelled by the exchange of a Reggeon \mathcal{B} .

In this kinematical regime, the process may be modelled as shown in Fig. 3, in which the exchanged object is a Reggeon \mathcal{B} with well-defined $SU(3)$ quantum numbers. With a polarised beam and target, this kinematics allows us to measure the structure function $g_1^{\mathcal{B}}$ of the exchanged Regge trajectory \mathcal{B} .

This is analogous to the measurement of the photon structure function g_1^γ in polarised e^+e^- scattering in the DIS region[7,8] (Fig. 4) or the pomeron structure function $F_2^{\mathcal{P}}$ in diffractive ep scattering[37] (Fig. 5).

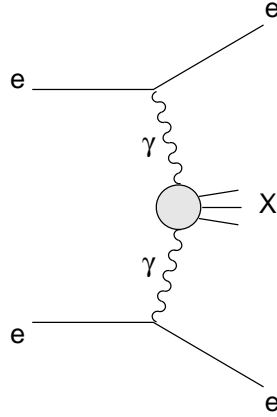


Fig.4 : The deep inelastic two-photon process in polarised e^+e^- scattering used to measure the structure function g_1^γ of the photon.

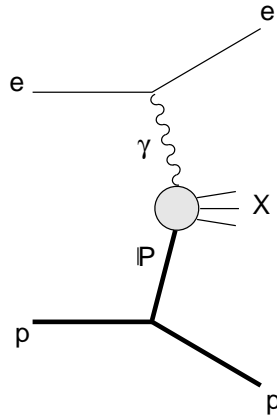


Fig.5 : The diffractive exchange process in ep scattering used to measure the structure function $F_2^{\mathcal{P}}$ of the pomeron.

Since the results of section 3 depend solely on the $SU(3)$ properties of the baryon \mathcal{B} , they will still hold here despite the fact that \mathcal{B} is interpreted as a Reggeon. Indeed, it is not even necessary (see section 4.2) to assume that the exchanged object is a single Reggeon – our final predictions for cross section ratios hold independently of the dynamical nature of the exchanged object, which could in principle be a multi-Regge exchange or more complicated structure, provided the $SU(3)$ properties are correct.

If the target is a nucleon N and the detected hadron is an octet meson (π), $SU(3)$ symmetry shows that \mathcal{B} belongs to a representation on the rhs of

$$\mathbf{8} \times \mathbf{8} = \mathbf{1} + \mathbf{8} + \mathbf{8} + \mathbf{10} + \bar{\mathbf{10}} + \mathbf{27} \quad (4.1)$$

Since the $\mathbf{27}$ requires a 5-quark state, it is a good dynamical approximation at sufficiently large z that the $\mathbf{10}$ dominates the $\mathbf{27}$. However, there is no such argument for $\mathbf{8}$ domi-

nance over the **10**. To isolate a unique representation for \mathcal{B} , we must therefore choose a combination of N and h giving I_3, Y quantum numbers for \mathcal{B} which appear in the **10** but not in the **8**. This is satisfied by the Δ^{++} and Δ^- , as in section 3. The required ratio of first moments $\Gamma_1^{\Delta^{++}}/\Gamma_1^{\Delta^-} = \frac{2s+2}{2s-1}$, where now Δ^{++} and Δ^- are Reggeons, is therefore obtained by comparing the reactions $ep \rightarrow e\pi^- X$ and $en \rightarrow e\pi^+ X$.

These symmetry considerations are easily pictured by drawing valence quark diagrams for the $Nh\mathcal{B}$ vertex. Fig. 6 shows the quark structure of the $ep \rightarrow e\pi^- X$ reaction, while the corresponding 5-quark, **27** representation, exchange is shown in Fig. 7.

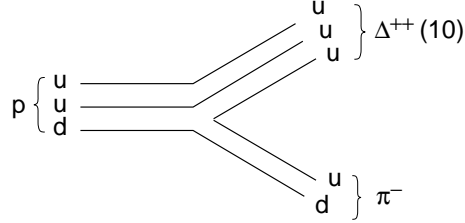


Fig.6 : Quark diagram for the $Nh\mathcal{B}$ vertex in the reaction $ep \rightarrow e\pi^- X$ with the Reggeon \mathcal{B} in the **10** representation.

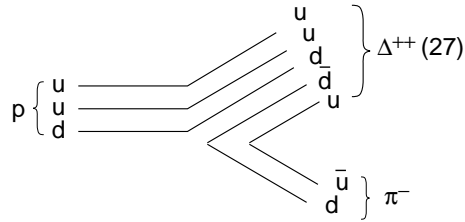


Fig.7 : Quark diagram for the $Nh\mathcal{B}$ vertex in the reaction $ep \rightarrow e\pi^- X$ with the Reggeon \mathcal{B} in the **27** representation.

As in section 3, we find the same ratio holds for the moments $\Gamma_1^{\Sigma_c^{++}}/\Gamma_1^{\Sigma_c^0}$, which can be realised (Fig. 8) in reactions in which a D meson is detected by comparing $ep \rightarrow eD^- X$ and $en \rightarrow eD^0 X$. To justify the assumption made there of treating the c quark as a spectator, we must select events in which there is no charmed jet in the current fragmentation region.

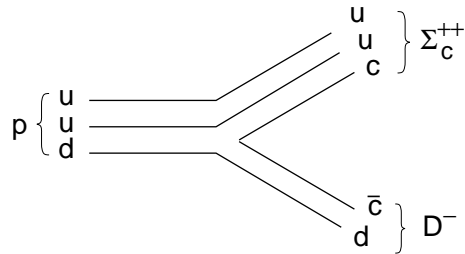


Fig.8 : Quark diagram for the $Nh\mathcal{B}$ vertex in the reaction $ep \rightarrow eD^- X$ where the Reggeon \mathcal{B} has quantum numbers of the Σ_c^{++} .

Trajectories with the quantum numbers of the Σ^+ and Σ^- would be exchanged in the reactions $ep \rightarrow eK^0 X$ and $en \rightarrow eK^+ X$ (substituting an s quark for the c quark in Fig. 8).

However, with these reactions there are two possibilities for the exchanged trajectory, with either the Σ^+ (Σ^-) in the **8** or the Σ^{*+} (Σ^{*-}) in the **10** being possible (in addition to the Zweig suppressed **27** contribution). As we saw in section 3, these give quite different ratios of structure function moments. Unfortunately, it would be difficult to distinguish these possibilities experimentally. In particular, there is no dynamical justification for assuming **10** dominance over the **8**. This is why we had to choose the Δ^{++} (Δ^-) or Σ_c^{++} (Σ_c^0) trajectories to obtain a clear test of the predictions of section 3.

The dynamics of these semi-inclusive reactions in the large z , target fragmentation region (Fig. 5) can be deduced by analogy with the photon structure function or diffractive pomeron exchange processes. The first moment of the polarised structure function for the Reggeon \mathcal{B} is found from the polarisation asymmetry of the differential cross section in the target fragmentation region, i.e.

$$\int_0^{1-z} dx x \frac{d\Delta\sigma^{target}}{dx dy dz dt} = \frac{Y_P}{2} \frac{4\pi\alpha^2}{s} \Delta f(z, t) \int_0^1 dx_{\mathcal{B}} g_1^{\mathcal{B}}(x_{\mathcal{B}}, t; Q^2) \quad (4.2)$$

Here, $x = \frac{Q^2}{2p_2 \cdot q}$, $x_{\mathcal{B}} = \frac{Q^2}{2k \cdot q}$, $z = \frac{p'_2 \cdot q}{p_2 \cdot q}$ so that $1 - z = \frac{x}{x_{\mathcal{B}}}$, $y = \frac{p_2 \cdot q}{p_2 \cdot p_1}$, $t = -(p_2 - p'_2)^2 \equiv -k^2$ and $Y_P = \frac{1}{y}(2 - y)$. This kinematics is described further in Appendix A.

If we now take the ratio of eq.(4.2) for the two reactions $ep \rightarrow e\pi^- X$ and $en \rightarrow e\pi^+ X$ (or $ep \rightarrow eD^- X$ and $en \rightarrow eD^0 X$), the factorised Reggeon emission factor $\Delta f(z, t)$ cancels out, leaving the ratio of structure function moments Γ_1 predicted in section 3 to be given simply by the ratio of the cross section moments. Our final predictions for the cross section ratios are summarised in section 4.3.

As well as predicting the ratios, which contain the essential physics we wish to test, we should also consider the absolute size of the relevant cross section asymmetries. In particular, we must check that the cross sections do not fall off too quickly as z approaches 1 for our predictions to be seen clearly in the data. Returning to eq.(4.2), and making the ansatz that the Reggeon emission factor $\Delta f(z, t)$ appropriate to the polarised amplitude is the same as that for the unpolarised case, we expect

$$\Delta f(z, t) \sim F(t)(1 - z)^{1 - 2\alpha_{\mathcal{B}}(t)} \quad (4.3)$$

where $\alpha_{\mathcal{B}}(t)$ is the Regge trajectory for the \mathcal{B} . For the reactions of interest, the relevant trajectory is the Δ , for which $\alpha_{\Delta}(t) \simeq 0.0 + 0.9t$, with t in GeV^2 . For the relevant experimental condition of t close to zero (corresponding to a small scattering angle θ_{LAB} of h relative to the incident nucleon in a collider experiment), the cross section moment therefore falls off only as $1 - z$.

4.2 Fracture Functions

Within the general framework of the parton model, the appropriate description of events in the target fragmentation region in semi-inclusive DIS is with fracture functions, introduced in ref.[10]. In this section, we show briefly how the fracture function description gives a more rigorous foundation to the results given in the previous section in terms of Reggeon structure functions.

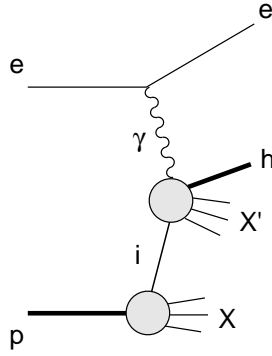


Fig.9 : The contribution to semi-inclusive DIS from the current fragmentation region.

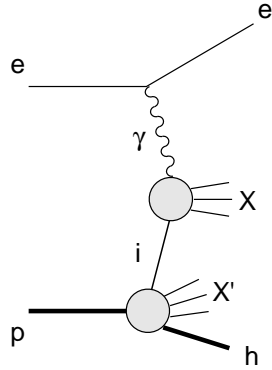


Fig.10 : The contribution to semi-inclusive DIS from the target fragmentation region.

The two distinct contributions to semi-inclusive DIS from the current and target fragmentation regions are shown in Figs. 9 and 10. The current fragmentation events are described by parton fragmentation functions $D_i^h(z; Q^2)$, where i denotes the parton, while the target fragmentation events are described by fracture functions $M_i^{hN}(x, z; Q^2)$ representing the joint probability distribution for producing a parton with momentum fraction x and a detected hadron h carrying energy fraction z from a nucleon N .

The differential cross section for polarised, semi-inclusive DIS has been given in refs.[38,39], including NLO corrections. (The equivalent results for the unpolarised case were calculated in ref.[40].) For our purposes here, we just quote the lowest order result:

$$x \frac{d\Delta\sigma}{dx dy dz} = \frac{Y_P}{2} \frac{4\pi\alpha^2}{s} \sum_i e_i^2 \left[\frac{1}{1-x} \Delta q_i(x; Q^2) D_i^h\left(\frac{z}{1-x}; Q^2\right) + \Delta M_i^{hN}(x, z; Q^2) \right] \quad (4.4)$$

where we have expressed the result in terms of the variable $z = \frac{p_2 \cdot q}{p_2 \cdot q}$ (see Appendix A). Here, $\Delta q_i(x; Q^2)$ and $\Delta M_i^{hN}(x, z; Q^2)$ are the polarisation asymmetries of the parton densities and fracture functions respectively. Restricting to the target fragmentation region, we simply have:

$$x \frac{d\Delta\sigma^{target}}{dx dy dz} = \frac{Y_P}{2} \frac{4\pi\alpha^2}{s} \sum_i e_i^2 \Delta M_i^{hN}(x, z; Q^2) \quad (4.5)$$

In the kinematical region $z \sim 1$ where the dominant process can be modelled as Reggeon exchange (Fig. 5), we can compare this expression to eq.(4.2). In this limit, therefore, we can relate the Reggeon structure function to the fracture function as follows:

$$\sum_i e_i^2 \int_0^{1-z} dx \Delta M_i^{hN}(x, z; Q^2) \underset{z \sim 1}{=} \int dt \Delta f(z, t) \int_0^1 dx_{\mathcal{B}} g_1^{\mathcal{B}}(x_{\mathcal{B}}, t; Q^2) \quad (4.6)$$

This is just the first moment of the more general relation

$$\sum_i e_i^2 \Delta M_i^{hN}(x, z; Q^2) \underset{z \sim 1}{=} \int dt \frac{1}{1-z} \Delta f(z, t) g_1^{\mathcal{B}}\left(\frac{x}{1-z}, t; Q^2\right) \quad (4.7)$$

This relation expresses the Reggeon structure function $g_1^{\mathcal{B}}$ in terms of its partonic constituents, as described by the fracture function ΔM_i^{hN} . We therefore see that the fracture function measures the parton distribution of the exchanged object[10]. Indeed, this interpretation is more general than the particular relation (4.7), since the fracture function description is not dependent on a particular model (such as a single Regge trajectory) for the exchanged object. For example, if the process is modelled by multi-Regge exchange, the rhs of eq.(4.7) would comprise a sum over the Reggeons.

We can take this identification a stage further by considering the extended fracture functions $M_i^{hN}(x, z, t; Q^2)$ introduced recently in ref.[11]. These are defined such that

$$M_i^{hN}(x, z; Q^2) = \int_0^{O(Q^2)} dt M_i^{hN}(x, z, t; Q^2) \quad (4.8)$$

where $t = -(p_2 - p'_2)^2$. Just as in the integrals of the Reggeon emission factors, the upper limit of the t integration is not precisely specified, with the physical results for large Q^2 being independent of the exact choice to the required order. These extended fracture functions have a number of important features[11], notably a much simpler, homogeneous, RG evolution equation. They also have an interesting interpretation in terms of spacelike cut vertices, whose RG properties are known to be determined by the anomalous dimensions of appropriate local operators.

These extended fracture functions allow us to remove the t integration in eq.(4.7), so we can finally write, to leading order,

$$\sum_i e_i^2 \Delta M_i^{hN}(x, z, t; Q^2) \underset{z \sim 1}{=} F(t)(1-z)^{-2\alpha_{\mathcal{B}}(t)} g_1^{\mathcal{B}}\left(\frac{x}{1-z}, t; Q^2\right) \quad (4.9)$$

where we have substituted eq.(4.3) for $\Delta f(z, t)$. The NLO corrections to the rhs of eq.(4.9) can be read off from refs.[38,39]. In fact, this should be taken as the definition of the ‘Reggeon structure function’ in the single Regge exchange approximation.

Since \mathcal{B} is a Reggeon, we cannot express the structure function $g_1^{\mathcal{B}}$ in terms of Wilson coefficients and operator matrix elements as for single particle structure functions such as g_1^p . Nevertheless, the moments of $g_1^{\mathcal{B}}$ should inherit a RG scaling dependence on the anomalous dimension of the appropriate OPE operator, e.g. A_μ^0 for the flavour singlet

first moment. For consistency, therefore, we would require the extended fracture function $\Delta M_i^{hN}(x, z, t; Q^2)$ to satisfy a homogeneous RG evolution equation. This is borne out by the results of ref.[11], where it is shown that

$$\frac{\partial}{\partial \ln Q^2} \Delta M_i^{hN}(x, z, t; Q^2) = \frac{\alpha_s(Q^2)}{2\pi} \int_x^{1-z} \frac{dw}{w} \Delta P_{ij}\left(\frac{x}{w}, \alpha_s(Q^2)\right) \Delta M_j^{hN}(w, z, t; Q^2) \quad (4.10)$$

where ΔP_{ij} is the usual DGLAP evolution kernel.

A satisfying picture therefore emerges, in which the results of section 4.1 are confirmed and placed in a broader theoretical framework for the description of semi-inclusive DIS.

4.3 Predictions

Of course, the ratio (3.6) is only obtained in the limit as z approaches 1, where the reaction $eN \rightarrow e h X$ is dominated by the process in which most of the target energy is carried through into the final state h by a single quark (see Figs. 6-8).

At the opposite extreme, for z approaching 0, the detected hadron carries only a small fraction of the target nucleon energy and has no special status compared to the other inclusive hadrons X . In this limit, therefore, the ratio of cross section moments (4.2) for $ep \rightarrow e\pi^- X$ and $en \rightarrow e\pi^+ X$ is simply the ratio of the structure function moments for the proton and neutron, i.e. Γ_1^p/Γ_1^n as given in section 3. The same result would hold for the ratio of $ep \rightarrow eD^- X$ and $en \rightarrow eD^0 X$.

We therefore predict the following results for the ratios of the differential cross section moments $\int_0^{1-z} dx x \frac{d\Delta\sigma^{target}}{dx dy dz dt}$:

$$\begin{aligned} \frac{en \rightarrow e\pi^+(D^0)X}{ep \rightarrow e\pi^-(D^-)X} &\sim \frac{2s-1}{2s+2} && (z \rightarrow 1) \\ &\sim \frac{2s+2-6sF/D}{2s-1-3(2s+1)F/D} && (z \rightarrow 0) \end{aligned} \quad (4.11)$$

Between these limits, we can only interpolate. We therefore expect a plot of the ratios of $\int_0^{1-z} dx x \frac{d\Delta\sigma^{target}}{dx dy dz dt}$ over the range $0 < z < 1$ for $en \rightarrow e\pi^+(D^0)X$ and $ep \rightarrow e\pi^-(D^-)X$ to look like the sketch in Fig. 11, where the solid line shows the ratios predicted by (4.11) with $s \sim 0.66$, contrasted with the ratios predicted by the OZI rule, i.e. $s = 1$ (dotted line).

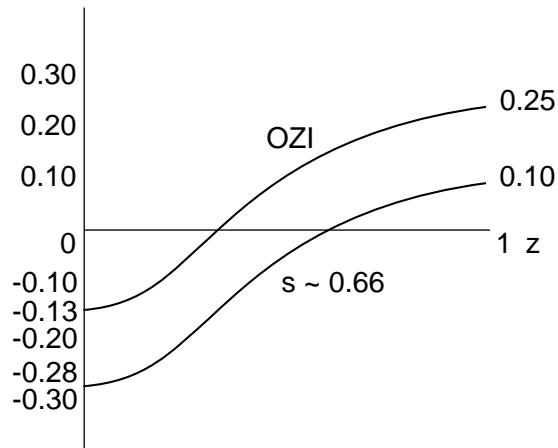


Fig.11 : Sketch of the cross section moment ratios for $en \rightarrow e\pi^+(D^0)X$ and $ep \rightarrow e\pi^-(D^-)X$, interpolating between the limits $z \rightarrow 0$ and $z \rightarrow 1$. The dotted line shows the OZI prediction and the solid line our prediction based on the target-independent suppression mechanism (with $s \sim 0.66$).

The difference between the OZI (or valence quark model) expectations and these predictions based on our target-independent interpretation of the ‘proton spin’ data is therefore quite dramatic, and should give a clear experimental signal.

Since our proposed experiment requires particle identification in the target fragmentation region, it is difficult to do at a polarised fixed-target experiment such as COMPASS[41] at CERN, which is better suited to studying semi-inclusive processes in the current fragmentation region. A better option is a polarised ep collider, such as HERA[42]. Testing our predictions requires comparison of proton and neutron data, which can be extracted from experiments with polarised deuterons replacing the protons in the collider.

Acknowledgements

The work of one of us (GMS) is partially supported by the EC TMR Network Grant FMRX-CT96-0008. We would like to thank R. Ball, D. de Florian, S. Forte, M. Grazzini, E-M. Kabuss, G. Mallot, S. Narison and L. Trentadue for helpful discussions.

Appendix A

A number of different definitions of the variable ‘ z ’ in semi-inclusive reactions are used in the literature. Here, we describe the relation between our notation and that used elsewhere, and present a number of useful kinematical results.

In refs.[38-40], the kinematics is described in the CM frame of the virtual photon and target nucleon. Let E_h and E_N be the energy of the detected hadron and nucleon in this frame and θ be the angle between the corresponding momenta. With the definition[40] $v = \frac{1}{2}(1 - \cos\theta)$, we see that the target fragmentation region is characterised by $v \sim 1$, while the current fragmentation region is $v \sim 0$. The hadron energy fraction variable used by ref.[40] is then

$$z_{(G)} = \frac{E_h}{E_N} \frac{1}{1-x} \quad (A.1)$$

In contrast, the corresponding variable used in refs.[34,35] is

$$z_h = \frac{p_2 \cdot p'_2}{p_2 \cdot q} \quad (A.2)$$

The relation is

$$z_h = z_{(G)}(1-v) \quad (A.3)$$

Notice[40] that these two variables are approximately equal in the current fragmentation region but differ substantially in the target fragmentation region, where z_h is small.

In terms of the variable $t = -(p_2 - p'_2)^2$, which in the model of Fig. 5 is the invariant spacelike momentum $-k^2$ of the exchanged Reggeon, we have

$$z_h = \frac{xt}{Q^2} \quad (A.4)$$

so that at fixed x, Q^2 in the target fragmentation region, z_h is simply a measure of t . The angle θ (assuming t is small compared to Q^2) is given by

$$\theta^2 \simeq \frac{4z}{x(1-x)} \frac{t}{Q^2} \quad (A.5)$$

Our preferred variable $z = \frac{p'_2 \cdot q}{p_2 \cdot q}$ can be expressed in this frame as

$$z = \frac{E_h}{E_N} - \frac{xt}{Q^2} = (1-x)z_{(G)} + O\left(\frac{t}{Q^2}\right) \quad (A.6)$$

so for relatively small t , z is simply given by the ratio of the detected hadron energy to the target nucleon energy in the photon-nucleon CM frame. The required kinematical region, where the semi-inclusive reaction is well approximated by the Reggeon exchange diagram and our prediction for the cross section moment ratios holds, is therefore $v \sim 1$ and z approaching 1.

References

- [1] G. Veneziano, *Mod. Phys. Lett. A4* (1989) 1605
- [2] G.M. Shore and G. Veneziano, *Phys. Lett. B244* (1990) 75
- [3] G.M. Shore and G. Veneziano, *Nucl. Phys. B381* (1992) 23
- [4] S. Narison, G.M. Shore and G. Veneziano, *Nucl. Phys. B433* (1995) 209
- [5] SMC Collaboration, hep-ex/9702005
E143 Collaboration, *Phys. Lett. B364* (1995) 61
- [6] SMC Collaboration (E-M. Kabuss), *to be published in Proceedings, QCD97 Montpellier*
SMC Collaboration (A. Magnon), *to be published in Proceedings, XVIII International Symposium on Lepton-Photon Interactions, Hamburg, July 1997*
- [7] S. Narison, G.M. Shore and G. Veneziano, *Nucl. Phys. B391* (1993) 69
- [8] G.M. Shore and G. Veneziano, *Mod. Phys. Lett. A8* (1993) 373
- [9] S.D. Bass, *Int. J. Mod. Phys. A7* (1992) 6039
- [10] L. Trentadue and G. Veneziano, *Phys. Lett. B323* (1994) 201
- [11] M. Grazzini, L. Trentadue and G. Veneziano, *in preparation*
- [12] S.G. Gorishny and S.A. Larin, *Phys. Lett. B172* (1986) 109
- [13] S.A. Larin and J.A.M. Vermaseran, *Phys. Lett. B259* (1991) 345
- [14] S.A. Larin, T. van Ritbergen and J.A.M. Vermaseran, *Phys. Lett. B404* (1997) 153
- [15] J. Kodaira, *Nucl. Phys. B165* (1980) 129
- [16] S.A. Larin, *Phys. Lett. B334* (1990) 1
- [17] D. Espriu and R. Tarrach, *Z. Phys. C16* (1982) 77
- [18] G. Altarelli and G.G. Ross, *Phys. Lett. B212* (1988) 391
- [19] R.D. Ball, S. Forte and G. Ridolfi, *Phys. Lett. B378* (1996) 255
- [20] R.D. Ball, *in Proceedings, Ettore Majorana International School of Nucleon Structure, Erice, 1995; hep-ph/9511330*
- [21] G.M. Shore, *Nucl. Phys. B (Proc. Suppl.) 39B,C* (1995) 101
- [22] G.M. Shore, *Nucl. Phys. B (Proc. Suppl.) 54A* (1997) 122
- [23] G.M. Shore and G. Veneziano, *Nucl. Phys. B381* (1992) 3
- [24] G.M. Shore, *to be published in Proceedings, QCD97 Montpellier*
- [25] G. Veneziano, *in 'From Symmetries to Strings: Forty Years of Rochester Conferences', ed. A. Das, World Scientific, 1990*
- [26] O. Alvarez and G.M. Shore, *Nucl. Phys. B213* (1983) 327
- [27] R.D. Ball, *Phys. Lett. B266* (1991) 473
- [28] B.L. Ioffe and A.Yu. Khodzhamiryan, *Yad. Fiz. 55* (1992) 3045
- [29] B.L. Ioffe, *in Proceedings, Ettore Majorana International School of Nucleon Structure, Erice, 1995; hep-ph/9511401*
- [30] B.V. Geshkenbein and B.L. Ioffe, *Nucl. Phys. B166* (1980) 340
- [31] V.A. Novikov, M.A. Shifman, A.I. Vainshtein and V.I. Zakharov, *Nucl. Phys. B191* (1981) 301
- [32] S. Narison, G.M. Shore and G. Veneziano, *in preparation*
- [33] G. Altarelli, R.D. Ball, S. Forte and G. Ridolfi, hep-ph/9701289
- [34] L.L. Frankfurt *et al.*, *Phys. Lett. B230* (1989) 141
- [35] SMC collaboration, *Phys. Lett. B369* (1996) 93

- [36] J.J. De Swart, Rev. Mod. Phys. 35 (1963) 916
- [37] T. Gehrmann and W.J. Stirling, Z. Phys. C70 (1996) 89
- [38] D. de Florian *et al.*, Nucl. Phys. B470 (1996) 195
- [39] D. de Florian, C.A. García Canal and R. Sassot, Phys. Lett. B389 (1996) 358
- [40] D. Graudenz, Nucl. Phys. B432 (1994) 351
- [41] COMPASS collaboration, CERN-SPSLC-96-14
- [42] G. Ingelman, A. De Roeck and R. Klanner (eds.), ‘Future Physics at HERA’, Proc., 1996 HERA Workshop